

TOWARDS TOUGH SELF-HEALING THIN-PLY LAMINATES

INSIGHTS FROM COMPUTATIONAL MICROMECHANICAL MODELING AND

HIGH-TEMPERATURE EXPERIMENTAL INVESTIGATION OF ONSET AND PROPAGATION OF
TRANSVERSE CRACKING

Luca Di Stasio^{1,2}

¹ Division of Materials Science, Luleå University of Technology, Luleå, Sweden

² EEIGM & IJL, Université de Lorraine, Nancy, France

Fundación para la Investigación, Desarrollo y Aplicación de Materiales Compuestos (FIDAMC)

Getafe, Madrid (ES) - September 16, 2019



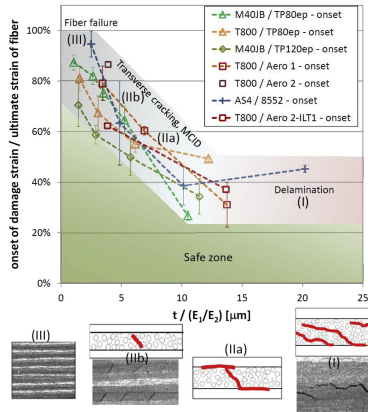
Outline

- ➔ Initiation of Transverse Cracks in Thin-plys
- ➔ Modeling the Fiber-Matrix Interface Crack
- ➔ Debond Energy Release Rate
- ➔ Conclusions

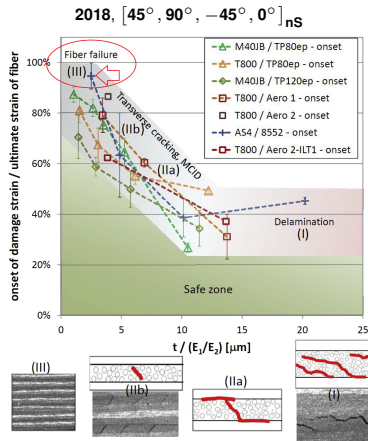


INITIATION OF TRANSVERSE CRACKS IN THIN-PLIES

The Thin-ply "Advantage": new material

2018, $[45^\circ, 90^\circ, -45^\circ, 0^\circ]$ nsCugnoni et al., Compos. Sci. Technol. **168**, 2018.

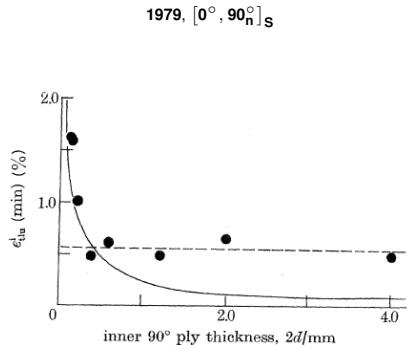
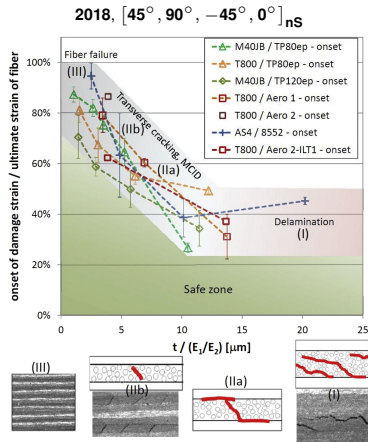
The Thin-ply "Advantage"? New material, new problem...



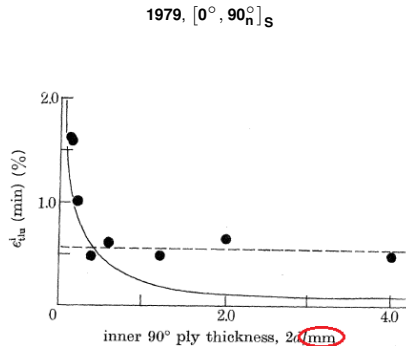
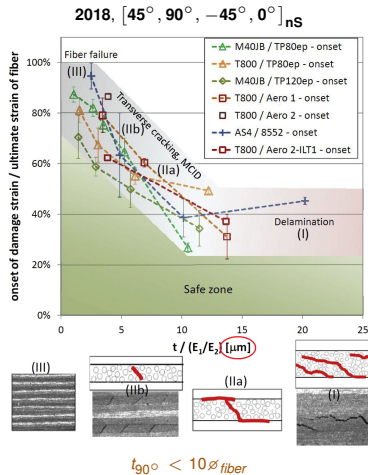
- material from NTPT (CH) (on the left)
- recent tests (master theses @ LTU) have shown the same behavior with material from Oxeon (SE)
- extended range of elastic behavior with no damage-induced stiffness reduction
- brittle failure of the whole laminate!
- very risky for application in safety-critical primary structures!

Cugnoni et al., Compos. Sci. Technol. **168**, 2018.

The Thin-ply "Advantage": new material, old result

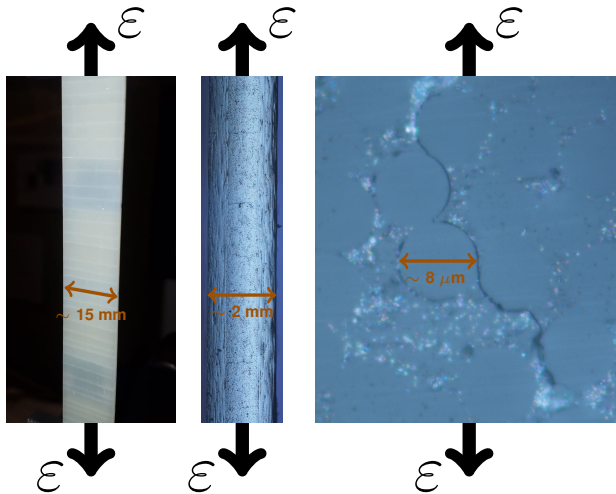


The Thin-ply "Advantage": new material, old result?



$t_{90^\circ} > 100 \phi_{fiber}$

Micromechanics of Initiation



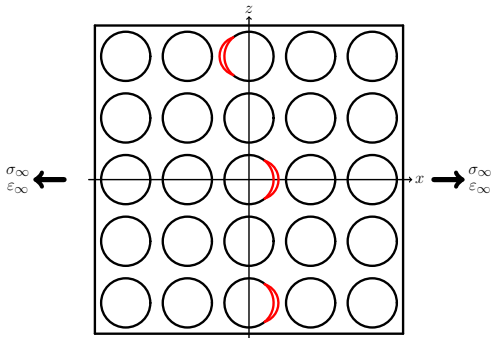
Left:
front view of $[0, 90]_S$,
visual inspection.

Center:
edge view of $[0, 90]_S$,
optical microscope.

Right:
edge view of $[0, 90]_S$,
optical microscope.

Micromechanics of Initiation

Stage 1: isolated debonds



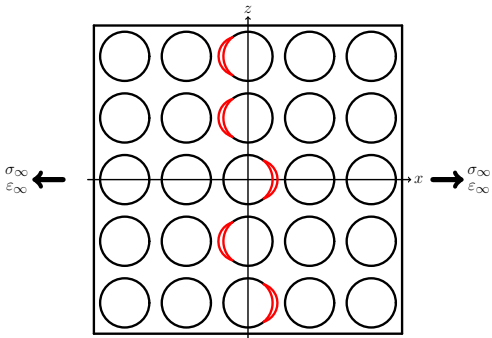
Bailey et al., P. Roy. Soc. A-Math. Phy. **366** (1727), 1979.

Bailey et al., J. Mater. Sci. **16** (3), 1981.

Zhang et al., Compos. Part A-Appl. S. **28** (4), 1997.

Micromechanics of Initiation

Stage 2: consecutive debonds



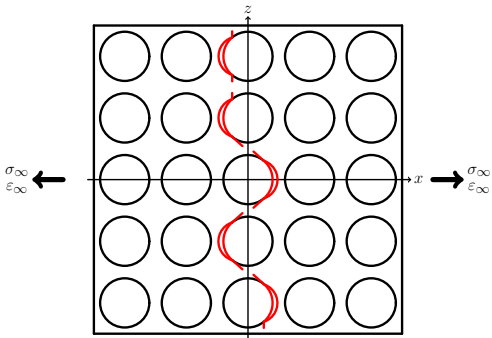
Bailey et al., P. Roy. Soc. A-Math. Phy. **366** (1727), 1979.

Bailey et al., J. Mater. Sci. **16** (3), 1981.

Zhang et al., Compos. Part A-Appl. S. **28** (4), 1997.

Micromechanics of Initiation

Stage 3: kinking



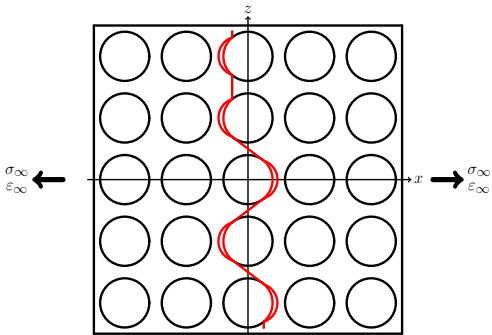
Bailey et al., P. Roy. Soc. A-Math. Phy. **366** (1727), 1979.

Bailey et al., J. Mater. Sci. **16** (3), 1981.

Zhang et al., Compos. Part A-Appl. S. **28** (4), 1997.

Micromechanics of Initiation

Stage 4: coalescence



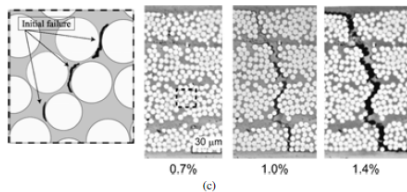
Bailey et al., P. Roy. Soc. A-Math. Phy. **366** (1727), 1979.

Bailey et al., J. Mater. Sci. **16** (3), 1981.

Zhang et al., Compos. Part A-Appl. S. **28** (4), 1997.

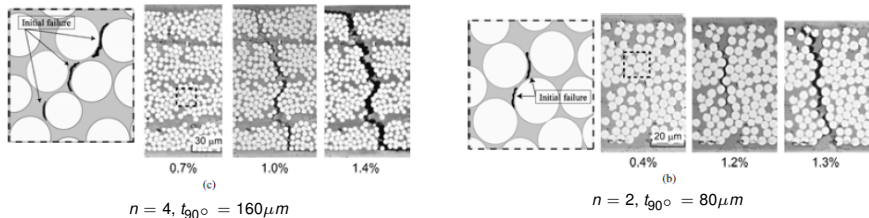
A Counter-intuitive Observation

[0°, 90°]_n



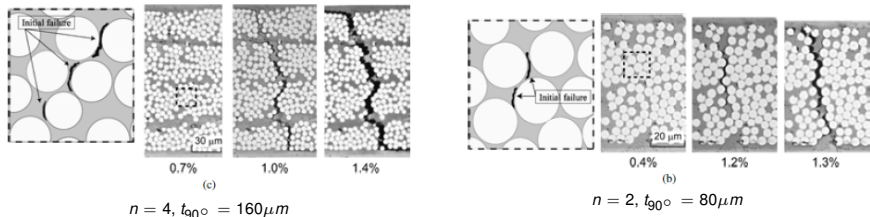
A Counter-intuitive Observation

$[0^\circ, 90_n^\circ]_S$



A Counter-intuitive Observation

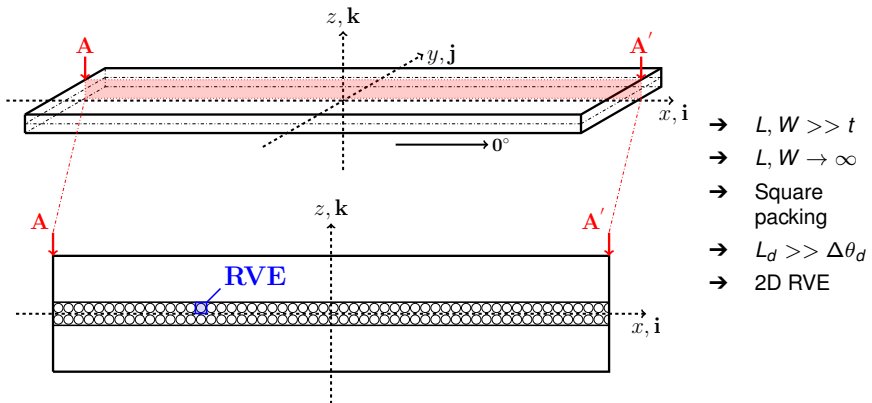
$[0^\circ, 90^\circ_n]_S$



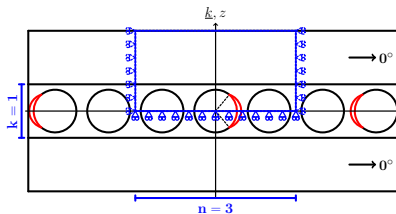
Saito et al., Adv. Compos. Mater. 21 (1), 2012.

MODELING THE FIBER-MATRIX INTERFACE CRACK

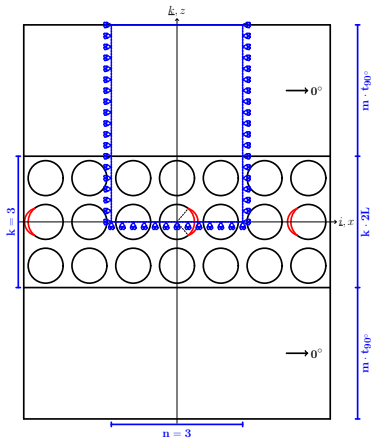
Geometry



Representative Volume Elements

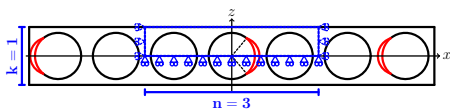


$$n \times 1 - m \cdot t_{90^\circ}$$



$$n \times k - m \cdot t_{90^\circ}$$

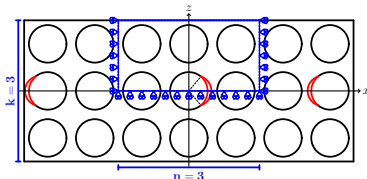
Representative Volume Elements



– free

$n \times 1$ – coupling

– coupling + H

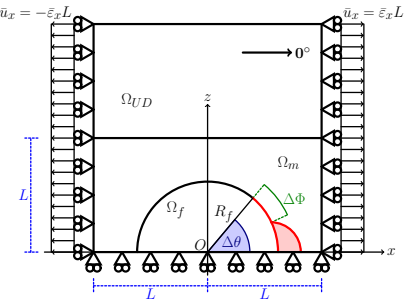


– free

$n \times k$ – coupling

– coupling + H

Assumptions

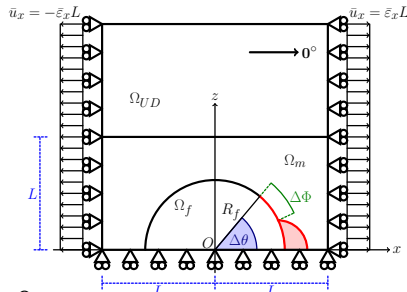


- Linear elastic, homogeneous materials
- Concentric Cylinders Assembly with Self-Consistent Shear Model for UD
- Plane strain
- Frictionless contact interaction
- Symmetric w.r.t. x-axis
- Coupling of x-displacements on left and right side (repeating unit cell)
- Applied uniaxial tensile strain $\bar{\varepsilon}_x = 1\%$
- $V_f = 60\%$

$$R_f = 1 \text{ } [\mu\text{m}] \quad L = \frac{R_f}{2} \sqrt{\frac{\pi}{V_f}}$$

Material	V_f [%]	E_L [GPa]	E_T [GPa]	μ_{LT} [GPa]	ν_{LT} [-]	ν_{TT} [-]
Glass fiber	-	70.0	70.0	29.2	0.2	0.2
Epoxy	-	3.5	3.5	1.25	0.4	0.4
UD	60.0	43.442	13.714	4.315	0.273	0.465

Solution



in Ω_f , Ω_m , Ω_{UD} :

$$\frac{\partial^2 \varepsilon_{xx}}{\partial z^2} + \frac{\partial^2 \varepsilon_{zz}}{\partial x^2} = \frac{\partial^2 \gamma_{zx}}{\partial x \partial z} \quad \text{for } 0^\circ \leq \alpha \leq \Delta\theta : \quad (\vec{u}_m(R_f, \alpha) - \vec{u}_f(R_f, \alpha)) \cdot \vec{n}_\alpha \geq 0$$

$$\varepsilon_y = \gamma_{xy} = \gamma_{yz} = 0$$

$$\frac{\partial \sigma_{xx}}{\partial x} + \frac{\partial \tau_{zx}}{\partial z} = 0$$

$$\frac{\partial \tau_{zx}}{\partial x} + \frac{\partial \sigma_{zz}}{\partial z} = 0$$

$$\sigma_{yy} = \nu(\sigma_{xx} + \sigma_{zz})$$

→ Oscillating singularity

$$\sigma \sim r^{-\frac{1}{2}} \sin(\varepsilon \log r), \quad V_f \rightarrow 0$$

$$\varepsilon = \frac{1}{2\pi} \log \left(\frac{1-\beta}{1+\beta} \right)$$

$$\beta = \frac{\mu_2(\kappa_1 - 1) - \mu_1(\kappa_2 - 1)}{\mu_2(\kappa_1 + 1) + \mu_1(\kappa_2 + 1)}$$

$$\rightarrow G = \frac{\partial W}{\partial A} - \left(\frac{\partial U}{\partial A} + \frac{\partial E_k}{\partial A} \right)$$

→ Finite Element Method (FEM)
in Abaqus™

→ 2nd order shape functions

→ 6-nodes triangles & 8-nodes quadrilaterals

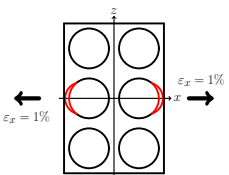
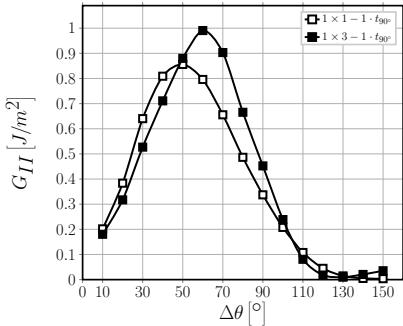
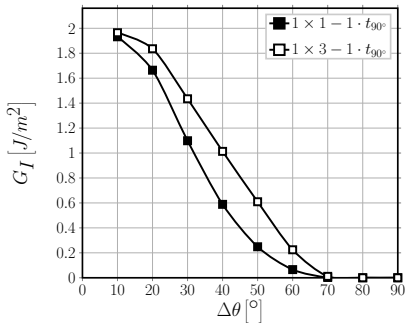
→ regular mesh of quadrilaterals
at the crack tip:

- $AR \sim 1$
- $\delta = 0.05^\circ$

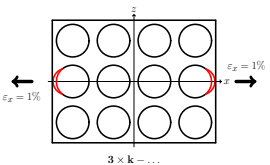
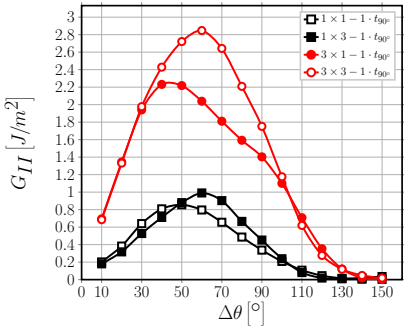
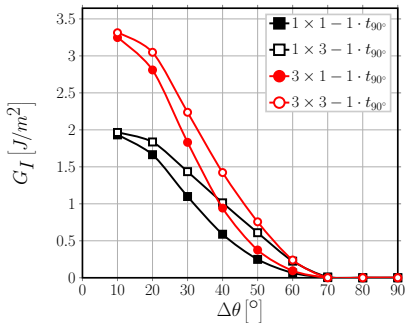
Initiation of Transverse Cracks in Thin-plies Modeling the Fiber-Matrix Interface Crack Debond Energy Release Rate Conclusions
Interaction of Debonds Effect of 0° ply thickness Effect of 90° ply thickness

DEBOND ENERGY RELEASE RATE

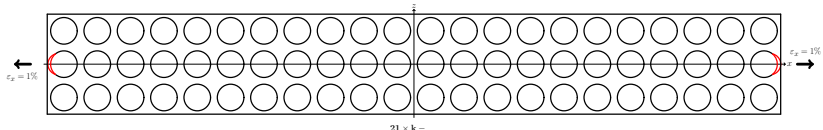
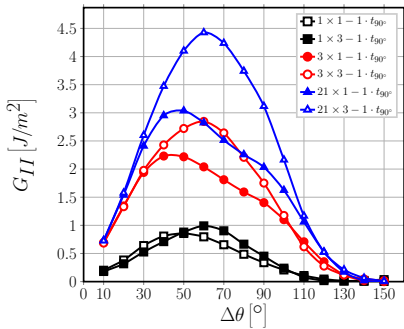
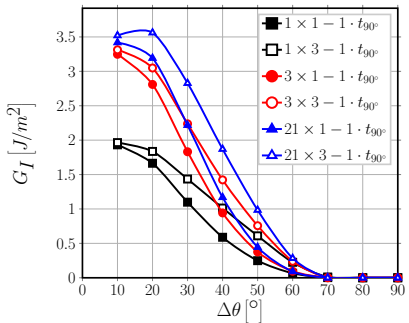
Interaction of Debonds: Strain Magnification



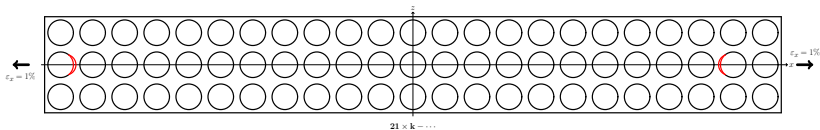
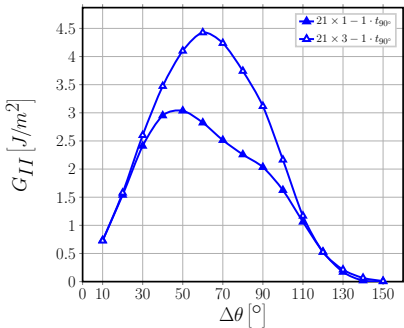
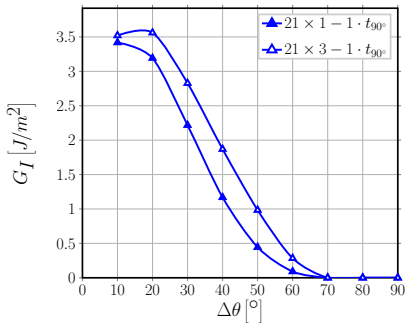
Interaction of Debonds: Strain Magnification



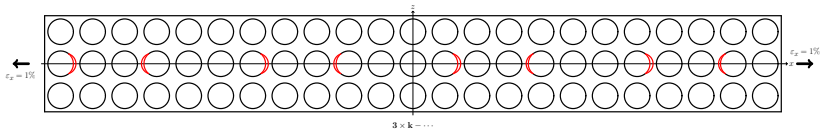
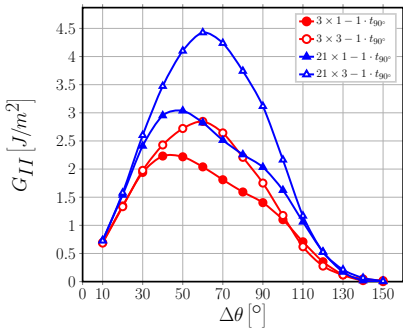
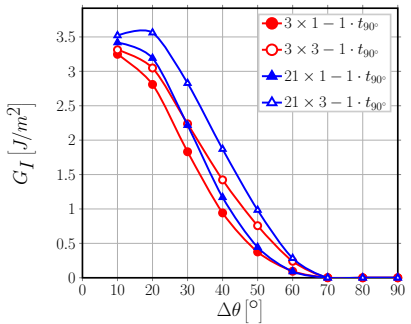
Interaction of Debonds: Strain Magnification



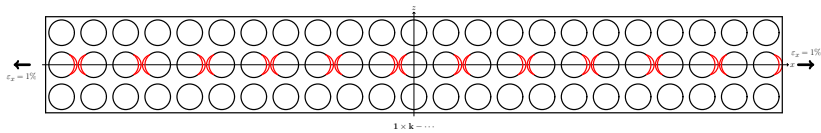
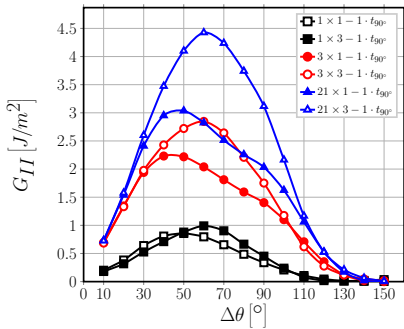
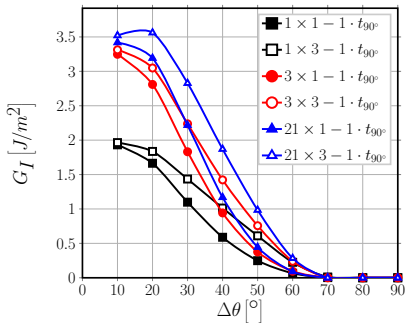
Interaction of Debonds: Crack Shielding



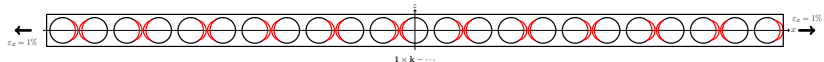
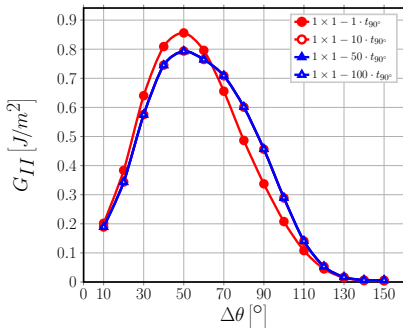
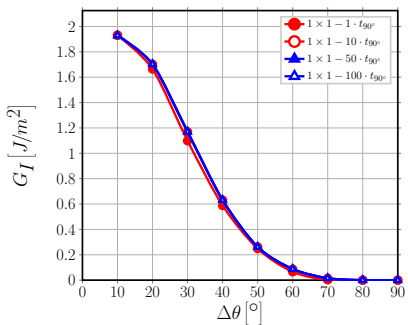
Interaction of Debonds: Crack Shielding



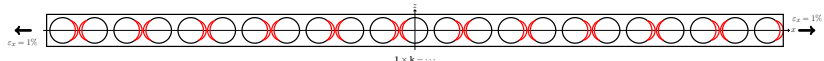
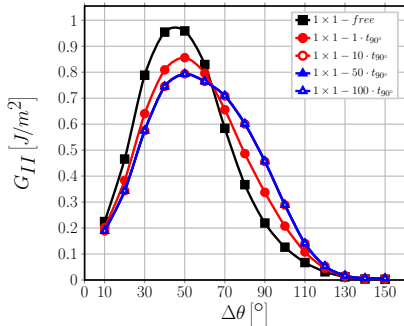
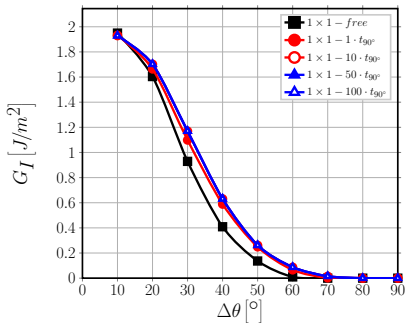
Interaction of Debonds: Crack Shielding



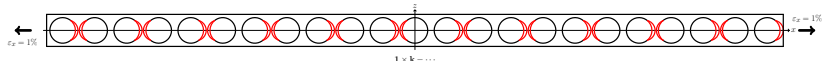
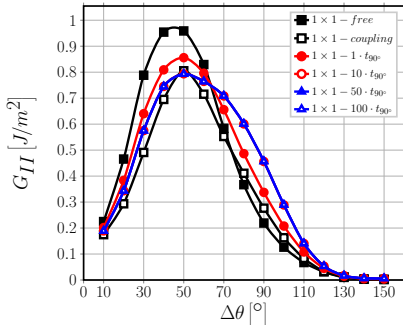
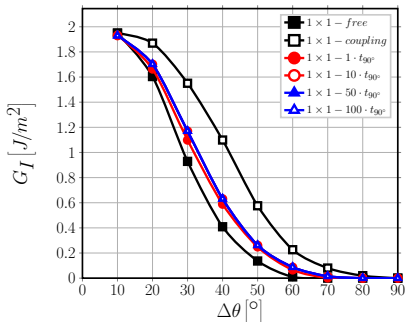
Effect of 0° ply thickness



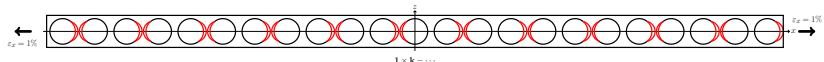
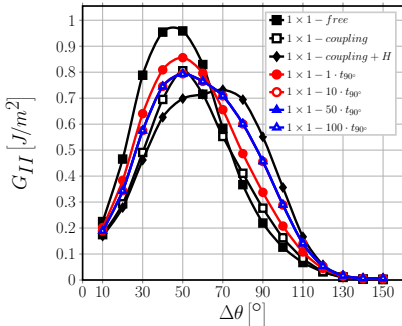
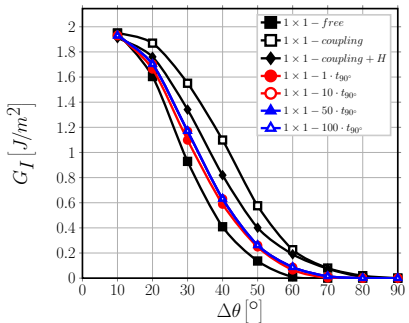
Effect of 0° ply thickness



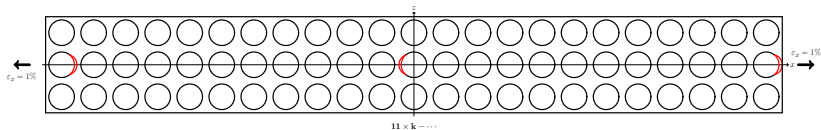
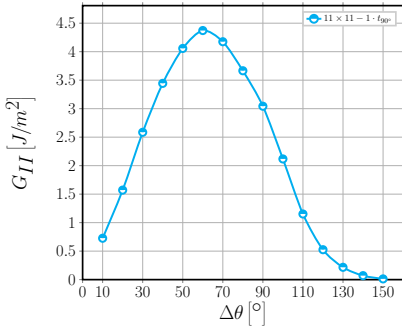
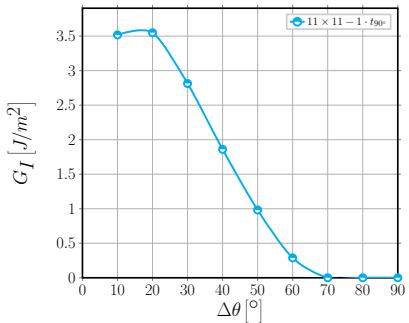
Effect of 0° ply thickness



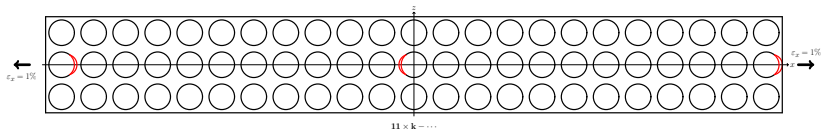
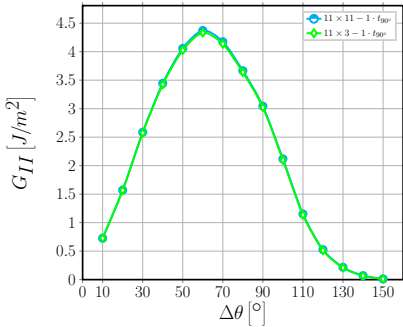
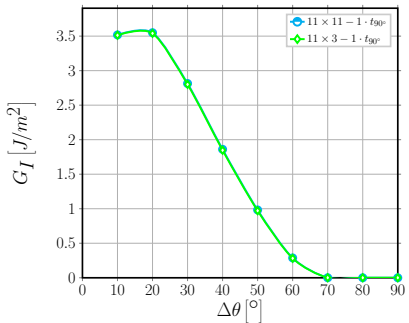
Effect of 0° ply thickness



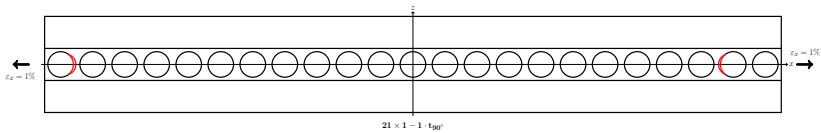
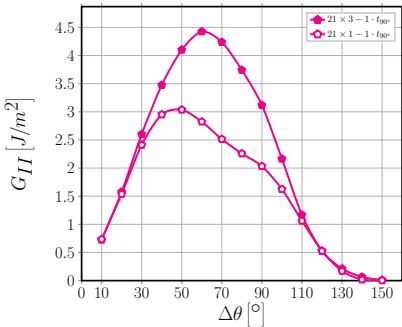
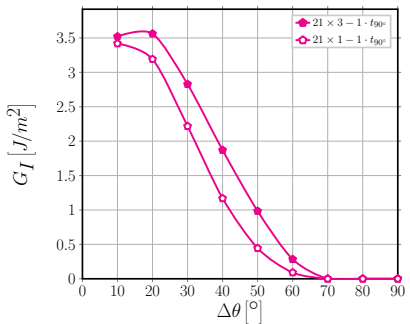
Effect of 90° ply thickness



Effect of 90° ply thickness



Effect of 90° ply thickness



CONCLUSIONS

Conclusions

- No effect of 90° ply thickness can be observed when t_{90° is at least $\sim 3\phi_{fiber}$
- Only if t_{90° is reduced to $1\phi_{fiber}$, ERR is reduced for a given level of applied strain, i.e. debond growth is delayed to higher levels of applied strain ($G \sim \varepsilon_{applied}^2$)
- No effect of 0° ply thickness can be observed when $t_{0^\circ}/t_{90^\circ} > 1$
- A small difference can be observed when $t_{0^\circ} = t_{90^\circ}$, due to the smaller bending stiffness of a thinner 0° layer

